

Constraints on Randall-Sundrum braneworld model from orbital motions

L. Iorio*

Long-range constraints on the AdS radius of curvature L in the Randall-Sundrum (RS) braneworld model are inferred from orbital motions of well known artificial and natural bodies. Thus, they do not rely upon more or less speculative and untested theoretical assumptions, contrary to other long-range RS tests proposed in astrophysical scenarios in which many of the phenomena adopted may depend on the system's composition, formation and dynamical history as well. The perihelion precession of Mercury and its radiotechnical ranging from the Earth yield $L \lesssim 10 - 50$ km. Tighter bounds come from the perigee precession of the Moon, from which it can be inferred $L \lesssim 500 - 700$ m. The best constraints ($L \lesssim 5$ m) come from the Satellite-to-Satellite Tracking (SST) range of the GRACE A/B spacecrafts orbiting the Earth: proposed follow-on of such a mission, implying a sub-nm s^{-1} range-rate accuracy, may constrain L at ~ 10 cm level. Weaker constraints come from the double pulsar system ($L \lesssim 80 - 100$ km) and from the main sequence star S2 orbiting the compact object in Sgr A* ($L \lesssim 6.2 - 8.8$ AU). Our results are valid also for other power-law interactions inducing potentials $U \propto r^{-3}$.

PACS numbers: 04.50.-h, 04.80.Cc, 95.10.Ce, 95.10.Km, 96.30.-t, 91.10.Sp

I. INTRODUCTION

Extra dimensions, arising in string theory, supergravity, M-theory [1] and string inspired higher dimensional theories such as the brane-world models [2–4], have recently gained increasing importance in physics in the context of the search for a quantum-gravity theory. In particular, large, non-compactified extra dimensions could potentially solve the long-lasting hierarchy problem [2, 3, 5, 6]. Indeed, if the standard model of particles and fields is restricted only on a (3+1)-dimensional brane, whereas gravity is allowed to propagate in the higher-dimensional bulk, the effective Planck scale in the four-dimensional spacetime can be made significantly larger than the electroweak scale, matching the experimental requirements.

In the braneworld model by Randall and Sundrum (RS hereafter) [3], our usual four-dimensional spacetime is a brane, which the standard model fields are constrained to, embedded in a five-dimensional anti-de Sitter (AdS) spacetime. In it, the fifth spatial dimension can be infinite, with an AdS curvature scale L . Indeed, the RS model circumvents the need of compactifying all but the three observed spatial dimensions by including a bound state of the massless graviton on the brane [3] resulting from the curvature, rather than the size, of the extra dimension. At distances $r \gg L$, the RS model implies a correction U_{RS} to the Newtonian gravitational potential of a body of mass M at second post-Newtonian order

(2PN). It is given by

$$U_{RS} = -k \frac{GM}{r} \left(\frac{L}{r} \right)^2, \quad (1)$$

where G is the Newtonian constant of gravitation, and k can assume different values depending on the schemes of regularization adopted [7]. E.g., it can be $k = 1$ [3], $k = 1/2$ [8], and $k = 2/3$ [9]. The occurrence of the correction of Eq. (1) to the Newtonian potential is important since, although it is only gravity that feels the presence of the extra dimensions, Eq. (1) allows for detectable effects on our (3+1)-brane that can be used in constraining the properties of the bulk.

Several large-scale tests of the RS model [3] have been proposed so far in astrophysical scenarios; they claimed bounds on L at $\sim 1 - 10 \mu\text{m}$ level, which is the same order of magnitude reached in laboratory-scale experiments [10]. Anyway, such constraints typically depend on the particular interpretation of astrophysical observations, and suffer from large systematic effects whose accurate knowledge is often lacking. Moreover, they are often quite model-dependent in the sense that they heavily rely upon theoretical assumptions which are still speculative since they have not yet been tested independently with a variety of different phenomena, or have not yet been directly tested at all. In our opinion, it is true also for those tests [11–14] requiring the least amount of information like, e.g., the evaporation of black holes [15]. Indeed, they are based on the application of a concept like the anti-de Sitter space/conformal field theory (AdS/CFT) duality [16] in braneworld gravity models that are asymptotically AdS (such as the RS models). Moreover, the consequent theoretical prediction for the black hole evaporation time [17–19] depends only on assumptions regarding the braneworld model and, in particular, on the validity and implementation of the AdS/CFT correspondence in view of the “no-hair” conjecture [20, 21], which is itself speculative and still awaits independent observational checks [22, 23]. Suffice it to say that the basis of

* Ministero dell'Istruzione, dell'Università e della Ricerca (M.I.U.R.)-Istruzione. Fellow of the Royal Astronomical Society (F.R.A.S.). International Institute for Theoretical Physics and Advanced Mathematics Einstein-Galilei. Permanent address: Viale Unità di Italia 68 70125 Bari (BA), Italy; lorenzo.iorio@libero.it

the previously cited calculation for the black hole evaporation time [17–19] has been recently challenged in Ref. [24]. In addition to such theoretical considerations at fundamental level, it must also be remarked that the astrophysical phenomena themselves used to constrain L , like the orbital evolution of black-hole X-Ray binaries or the behavior of black holes in extragalactic clusters, are not lacking of uncertainties, both from a theoretical and observational point of view. E.g., they may crucially depend on the composition, formation and dynamical history of the systems considered. Last but not least, black holes may well not exist at all [25, 26]; e.g., even in the case of the compact object in Sgr A*, there are not yet direct evidences that its $\sim 10^6 M_\odot$ mass is actually concentrated within its Schwarzschild radius $R_s = 0.084$ AU [27]. A signature for the absence of event horizons was even looked for by the authors of Ref. [28]. In conclusion, to date, a definite proof for the existence of Kerr black holes is still lacking despite a wealth of observational evidence [29].

Thus, in Sec. II we will use well known and largely tested orbital motions (see Sec. IIA) of some natural (Sec. IIB) and artificial (Sec. IIC) bodies in the solar system to infer constraints on the AdS radius of curvature which, if on the one hand, are not at μm level, on the other hand can certainly be considered less speculative than those obtained in astrophysical contexts. Indeed, apart from the fact that there are no doubts about the existence and the properties of the planets of the solar system and of man-made Earth’s satellites, the dynamical effects used to constrain L are straightforwardly obtained from Eq. (1), without any additional hypothesis concerning untested phenomena. Moreover, competing effects acting as systematic errors are known with a comparatively much better accuracy. We notice that McWilliams [30] recently proposed to constrain L via gravitational wave measurements in the solar system: LISA would allow to place bounds on the AdS radius of curvature of the order of $L \sim 1 \mu\text{m}$ from the event rate of stellar black holes inspiraling gravitationally into supermassive black holes, and of $L \lesssim 5 \mu\text{m}$ from the observation of individual galactic binaries containing a stellar mass black hole. In Sec. IID we will also use the well known, and extensively studied, double pulsar binary system and the main sequence S2 star orbiting the compact object in Sgr A*. Finally, we stress that our results are not necessarily limited to the RS model [3], being valid also for other theoretical schemes yielding power-law interactions $\propto r^{-3}$ [10, 31].

II. RS LONG-TERM ORBITAL EFFECTS AND COMPARISON WITH THE OBSERVATIONS

A. Analytical calculation of the secular precession of the pericenter

The long-period effects caused by Eq. (1) on the orbital motion of a test particle of mass m can be computed perturbatively by adopting the Lagrange equations for the variation of the osculating Keplerian elements [32]: their validity has been confirmed in a variety of independent phenomena. Generally speaking, they imply the use of a perturbing function \mathcal{R} which is the correction U_{pert} to the standard Newtonian monopole term. In the case $U_{\text{pert}} = U_{\text{RS}}$, the average over one orbital revolution of the perturbing function \mathcal{R} is straightforwardly obtained by using the true anomaly f as fast variable of integration: it is

$$\langle \mathcal{R} \rangle = -\frac{GMkL^2}{a^3(1-e^2)^{3/2}}, \quad (2)$$

where a is the semimajor axis and e is the eccentricity of the test particle’s orbit. From Eq. (2) and the Lagrange equation for variation of the longitude of pericenter ϖ [33]

$$\left\langle \frac{d\varpi}{dt} \right\rangle = -\frac{1}{n_b a^2} \left\{ \left[\frac{(1-e^2)^{1/2}}{e} \right] \frac{\partial \langle \mathcal{R} \rangle}{\partial e} + \frac{\tan(I/2)}{(1-e^2)^{1/2}} \frac{\partial \langle \mathcal{R} \rangle}{\partial I} \right\}, \quad (3)$$

it turns out that ϖ experiences a secular precession given by

$$\left\langle \frac{d\varpi}{dt} \right\rangle = \frac{3(GM)^{1/2} kL^2}{a^{7/2}(1-e^2)^2}. \quad (4)$$

In Eq. (3), $n_b \doteq \sqrt{GM/a^3}$ is the Keplerian mean motion and I is the inclination of the orbital plane to the reference $\{x, y\}$ plane. The longitude of pericenter $\varpi \doteq \Omega + \omega$ is a “dogleg” angle since it is the sum of the longitude of the ascending node Ω , which is an angle in the reference $\{x, y\}$ plane from a reference x direction to the intersection of the orbital plane with the $\{x, y\}$ plane itself (the line of the nodes), and of the argument of pericenter ω , which is an angle counted in the orbital plane from the line of the nodes to the point of closest approach, usually dubbed pericenter. The precession of Eq. (4), which is an exact result in the sense that no a-priori assumptions on e were made, agrees with the one obtained by Adkins and McDonnell in Ref. [34] with a more cumbersome calculation. To facilitate a comparison between such two results, we note that, in general, the authors of Ref. [34] work out the perihelion advance per orbit $\Delta\theta_p$: it corresponds to $\langle \dot{\varpi} \rangle P_b$, where $P_b = 2\pi/n_b$ is the orbital period. Moreover, in the potential energy $V(r) = \alpha_{-(j+1)} r^{-(j+1)}$ it must be posed $j = 2$ and $\alpha_{-3} \rightarrow -GMmkL^2$, while in $\Delta\theta_p(-(j+1))$ of Eq. (38) in Ref. [34] it must be set $L \rightarrow a(1-e^2)$, $\chi_2(e) = 6$. With such replacements, it

can be shown that the advance per orbit of Eq. (38) in Ref. [34] corresponds just to our precession in Eq. (4). Moreover, the analytical result of Eq. (4) is confirmed by a numerical integration of the equations of motion for Mercury with, say, $L = 10^{-6}$ AU and $k = 1/2$ displayed in Figure 1: both yield 5.4 milliarcseconds per century (mas cty^{-1} hereafter). The choice of the numerical value adopted for L is purely arbitrary, being motivated only by the need of dealing with relatively small numbers.

B. Constraints from solar system planetary orbital motions

The corrections $\Delta\dot{\omega}$ to the standard Newtonian-Einsteinian secular precessions of the longitudes of the perihelia are routinely used by independent teams of astronomers [35, 36] as a quantitative measure of the maximum size of any putative anomalous effect allowed by the currently adopted mathematical models of the standard solar system dynamics fitted to the available planetary observations. Thus, $\Delta\dot{\omega}$ can be used to put constraints on the parameters like L entering the exotic models one is interested in. From Eq. (4) it turns out that the tightest constraints come from Mercury, which is the innermost planet with $a = 0.38$ AU, for $k = 1$.

Fienga et al. [36], who used also a few data from the three flybys of MESSENGER in 2008-2009, released an uncertainty of 0.6 mas cty^{-1} for the perihelion precession of Mercury, so that it is $L \lesssim 34 - 48 \text{ km}$ for $k = 1 - 1/2$. The uncertainty in the pre-MESSENGER Mercury's perihelion extra-precession by Pitjeva [35] is about one order of magnitude larger (5 mas cty^{-1}).

Slightly tighter constraints on L come from the interplanetary Earth-Mercury ranging. Indeed, according to Table 1 of Ref. [36], the standard deviation $\sigma_{\Delta\rho}$ of the Mercury range residuals $\Delta\rho$, obtained with the INPOP10a ephemerides and including also three Mercury MESSENGER flybys in 2008-2009, is as large as 1.9 m. A numerical integration of the equations of motion of Mercury and the Earth yields a RS range signal with the same standard deviation for $L \lesssim 13 - 18 \text{ km}$ ($k = 1 - 1/2$). Figure 2 displays the case $k = 1/2$. It turns out that the residuals of right ascension (RA) and declination (DEC) in Ref. [36] yield much less tight constraints.

As far as natural bodies of the solar system are concerned, the Moon yields better results. Its orbit is accurately reconstructed with the Lunar Laser Ranging (LLR) technique [37] since 1969; Figure B-1 of Ref. [38] shows that the residuals of the Earth-Moon range are at a cm-level since about 1990. The secular precession of the lunar perigee is known with an accuracy of about 0.1 mas yr^{-1} [39–42], so that Eq. (4) yields $L \lesssim 524 - 741 \text{ m}$ ($k = 1 - 1/2$).

C. Constraints from the GRACE spacecraft orbiting the Earth

Remaining within the solar system, tighter constraints can be obtained from selected spacecrafts orbiting the Earth. The Gravity Recovery and Climate Experiment (GRACE) mission [43], jointly launched in March 2002 by NASA and the German Space Agency (DLR) to map the terrestrial gravitational field with an unprecedented accuracy, consists of a tandem of two spacecrafts moving along low-altitude, nearly polar orbits continuously linked by a Satellite to Satellite Tracking (SST) microwave K-band ranging (KBR) system accurate to better than $10 \mu\text{m}$ (biased range ρ) [44] and $1 \mu\text{m s}^{-1}$ (range-rate $\dot{\rho}$) [44, 45]. Studies for a follow-on of GRACE show that the use of an interferometric laser ranging system may push the accuracy in the range-rate to a $\sim 0.6 \text{ nm s}^{-1}$ level. A numerical integration of the equations of motion for GRACE A/B, including also the mismodelled signal of the first nine zonal harmonics of geopotential [32] according to the global Earth gravity model GOCO01S [47], shows that the SST range is more effective than the SST range-rate in constraining the RS parameter for which it holds $L \lesssim 5 \text{ m}$. Figure 3 depicts the numerically integrated GRACE SST range signal due to Eq. (1) and the aforementioned mismodelled zonals. It can be shown that a sub-nm s^{-1} level of accuracy in the GRACE SST range-rate would imply the possibility of constraining L down to $\sim 10 \text{ cm}$ level.

D. Constraints from the double pulsar and Sgr A*

Constraints comparable with the planetary ones can be obtained from the periastron of the double pulsar PSR J0737-3039A/B system [48, 49]. Indeed, the semimajor axis of its relative orbit amounts to just $a = 0.006 \text{ AU}$ [50]. The present-day accuracy in measuring the secular precession of the periastron is $6.8 \times 10^{-4} \text{ deg yr}^{-1}$ in the following [50]; thus, a straightforward application of it to Eq. (4) would give $L \lesssim 11 - 16 \text{ km}$ ($k = 1 - 1/2$). Actually, the larger uncertainty in the theoretical expression of the general relativistic 1PN periastron precession must be taken into account as well. It is as large as 0.03 deg yr^{-1} [51], so that it yields $L \lesssim 80 - 112 \text{ km}$ ($k = 1 - 1/2$).

The perinigricon of the S2 star, orbiting in 15.98 yr the compact object hosted in Sgr A* with $M = 4 \times 10^6 M_\odot$ [52] at $\langle r \rangle = 1433 \text{ AU}$ from it [53], yields much weaker constraints on the asymptotic AdS curvature. Indeed, an accuracy of [53] 0.05 deg yr^{-1} can be inferred for the perinigricon precession of S2: thus, $L \lesssim 6.2 - 8.8 \text{ AU}$.

[1] J. Polchinski, String Theory (Cambridge University Press, Cambridge, England, 1998), Vols. I and II.

[2] L. Randall and R. Sundrum, Phys. Rev. Lett. **83**, 3370

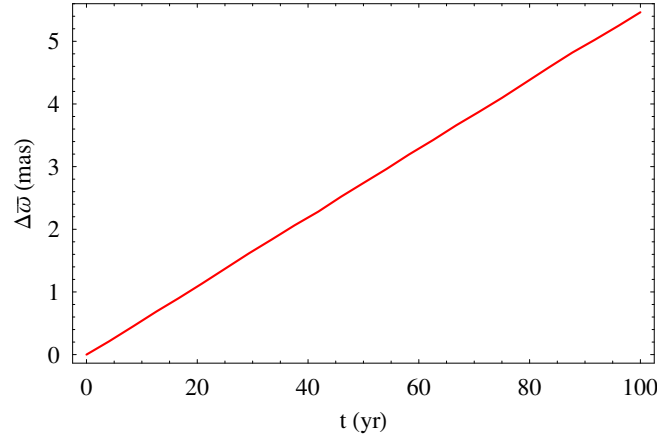
RS shift of Mercury's longitude of perihelion ($L = 10^{-6}$ AU, $k = 1/2$)

FIG. 1. Centennial shift $\Delta\omega$, in mas, of the longitude of perihelion of Mercury due to the RS potential of Eq. (1) for $L = 10^{-6}$ AU and $k = 1/2$ computed from the difference between two numerical integrations of the equations of motion in cartesian coordinates performed with and without Eq. (1). Both the integrations share the same initial conditions, retrieved from the NASA WEB interface HORIZONS at <http://ssd.jpl.nasa.gov/horizons.cgi>, for the epoch J2000.0. It agrees with the analytical result from Eq. (4).

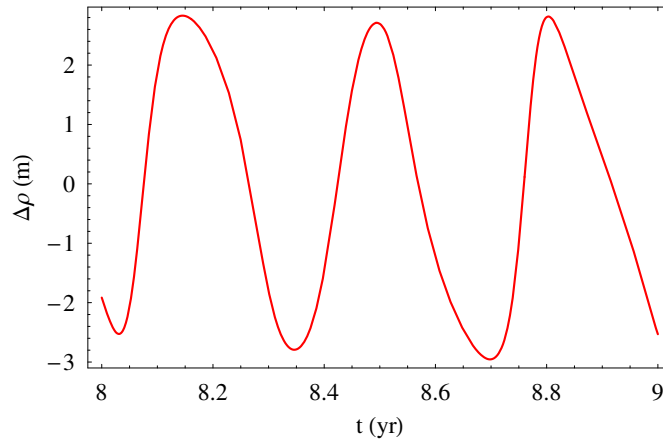
Earth–Mercury RS range perturbation ($L = 18$ km, $k = 1/2$)

FIG. 2. 2008-2009 Earth-Mercury range shift $\Delta\rho$, in m, due to the unmodeled RS potential of Eq. (1) for $L = 18$ km and $k = 1/2$ computed from the difference between two numerical integrations of the equations of motion in cartesian coordinates performed with and without Eq. (1). Both the integrations share the same initial conditions retrieved from the NASA WEB interface HORIZONS at <http://ssd.jpl.nasa.gov/horizons.cgi>, for the epoch J2000.0. It is $\langle\Delta\rho\rangle = -0.04$ m, $\sigma_{\Delta\rho} = 1.9$ m.

- (1999).
- [3] L. Randall and R. Sundrum, Phys. Rev. Lett. **83**, 4690 (1999).
 - [4] T. Shiromizu, K.-I. Maeda, and M. Sasaki, Phys. Rev. D **62**, 024012 (2000).
 - [5] N. Arkani-Hamed, S. Dimopoulos, and G. Dvali, Phys. Lett. B **429**, 263 (1998).
 - [6] I. Antoniadis, N. Arkani-Hamed, S. Dimopoulos, and G. R. Dvali, Phys. Lett. B **436**, 257 (1998).
 - [7] E. Jung, S. H. Kim, and D. K. Park, Nucl. Phys. B **669**, 306 (2003).
 - [8] A. O. Barvinsky, Phys. Usp. **48**, 6 (2005).
 - [9] J. Garriga and T. Tanaka, Phys. Rev. Lett. **84**, 2778 (2000).
 - [10] E. G. Adelberger, B.R. Heckel, S. Hoedl, C. D. Hoyle, D. J. Kapner, and A. Upadhye, Phys. Rev. Lett. **98**, 131104 (2007).
 - [11] D. Psaltis, Phys. Rev. Lett. **98**, 181101 (2007).
 - [12] O. Y. Gnedin, T. J. Maccarone, D. Psaltis, and S. E. Zepf, Astrophys. J. Lett. **705**, L168 (2009).
 - [13] T. Johannsen, D. Psaltis, and J. E. McClintock, **691**, 997 (2009).
 - [14] T. Johannsen, Astron. Astrophys. **507**, 617 (2009).
 - [15] J. Traschen, in *Mathematical Methods in Physics*, edited by A. Bytsenko and F. L. Williams (World Scientific, Singapore, 2000), p. 180.
 - [16] O. Aharony, S. S. Gubser, J. Maldacena, H. Ooguri, and Y. Oz, Phys. Rept. **323**, 183 (2000).
 - [17] R. Emparan, J. García-Bellido, and N. Kaloper, J. High Energy Phys. **1** (2003) 79.

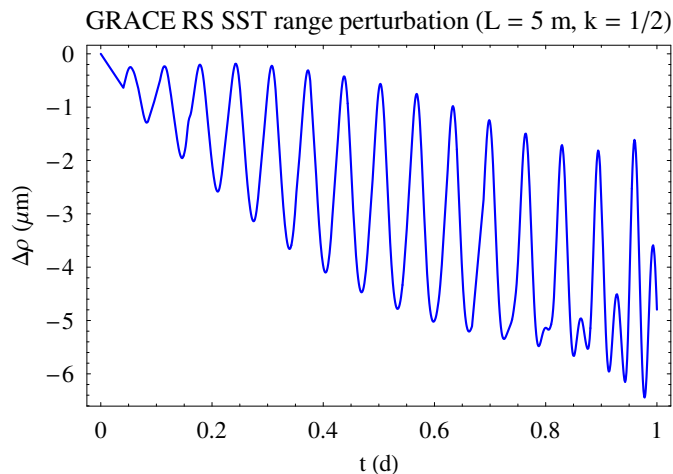


FIG. 3. Daily GRACE SST range shift $\Delta\rho$, in μm , due to the unmodeled RS potential of Eq. (1) ($L = 5 \text{ m}$, $k = 1/2$) and the first nine mismodelled zonals of geopotential according to GOCO01S [47] computed from the difference between two numerical integrations of the equations of motion in cartesian coordinates performed with and without the perturbations considered. Both the integrations share the same initial conditions contained in the files GNV1B_2003-09-14_A.00 and GNV1B_2003-09-14_B.00 retrieved from ftp://cddis.gsfc.nasa.gov/pub/slr/predicts/current/graceA_irvs_081202_0.gfz and ftp://cddis.gsfc.nasa.gov/pub/slr/predicts/current/graceB_irvs_081201_1.gfz. The epoch is 13 September 2003. (See ftp://podaac.jpl.nasa.gov/pub/grace/doc/Handbook_1B.v1.3.pdf for the explanation of the GPS Navigation Data Format Record (GNV1B) format). It is $\langle\Delta\rho\rangle = -3 \mu\text{m}$, $\sigma_{\Delta\rho} = 2 \mu\text{m}$.

- [18] T. Tanaka, Prog. Theor. Phys. Suppl. **148**, 307 (2003).
- [19] R. Emparan, A. Fabbri, and N. Kaloper, J. High Energy Phys. **08** (2002) 042.
- [20] P. T. Chrusciel, Contemp. Math. **170**, 23 (1994).
- [21] M. Heusler, Living Rev. Rel. **1**, 6. (1998).
- [22] C. M. Will, Astrophys. J. **674**, L25 (2008).
- [23] T. Johansson, Adv. Astron. **2012**, 486750 (2012).
- [24] A. L. Fitzpatrick, L. Randall, and T. Wiseman, J. High Energy Phys. **11** (2006) 033.
- [25] P. Ball, Nature doi:10.1038/news050328-8 (2005).
- [26] G. Chapline, in *Proceedings of the 22nd Texas Symposium on Relativistic Astrophysics at Stanford. eConf: C041213*, edited by P. Chen, E. Bloom, G. Madejski, and V. Patrosian (Stanford University, Stanford, 2005) p. 101.
- [27] A. Balbi, *Elementi di Astrofisica 2, Lezione 13* (Università degli studi di Roma “Tor Vergata”, Rome, 2010), p. 18.
- [28] J. Barbieri and G. Chapline, arXiv:0812.0833 (2008).
- [29] D. Psaltis, *Compact Stellar X-Ray Sources* (Cambridge University Press, Cambridge, 2006).
- [30] S. T. McWilliams, Phys. Rev. Lett. **104**, 141601 (2010).
- [31] F. Ferrer and J. A. Grifols, Phys. Rev. D **58**, 096006 (1998).
- [32] M. Capderou, *Satellites* (Springer, Paris, 2005), p. 80.
- [33] B. Bertotti, P. Farinella, D. Vokrouhlický, *Physics of the Solar System* (Kluwer, Dordrecht, 2003), p. 324.
- [34] G. S. Adkins and J. McDonnell, Phys. Rev. D **75**, 082001 (2007).
- [35] E. V. Pitjeva, in *Proceedings of the International Astronomical Union, 5*, edited by S. A. Klioner, P. K. Seidelman and M. H. Soffel (Cambridge University Press, Cambridge, 2009), p. 170.
- [36] A. Fienga, J. Laskar, P. Kuchynka, H. Manche, G. Desvignes, M. Gastineau, I. Cognard, and G. Theureau, Celest. Mech. Dyn. Astron. **111**, 363 (2011).
- [37] J. O. Dickey, P. L. Bender, J. E. Faller, X. X. Newhall, R. L. Ricklefs, J. G. Ries, P. J. Shelus, C. Veillet, A. L. Whipple, J. R. Wiant et al., Science **265**, 482 (1994).
- [38] W. M. Folkner, J. G. Williams, and D. H. Boggs, *The planetary and lunar ephemeris DE 421, Memorandum IOM 343R-08-003* (Jet Propulsion Laboratory, California Institute of Technology, 2008).
- [39] J. Müller, M. Schneider, M. Soffel and H. Ruder, Astrophys. J. **382**, L101 (1991).
- [40] J. G. Williams, X. X. Newhall, and J. O. Dickey, Phys. Rev. D **53**, 6730 (1996).
- [41] J. Müller, J. G. Williams, S. G. Turyshev, and P. J. Shelus, in *Dynamic Planet*, edited by P. Tregoning and C. Rizos (Springer, Berlin, 2007), p. 903.
- [42] J. Müller, J. G. Williams, and S. G. Turyshev, in *Lasers, Clocks and Drag-Free Control*, edited by H. Dittus, C. Lämmerzahl, and S. G. Turyshev (Springer, Berlin, 2008), p. 457.
- [43] B. D. Tapley, S. Bettadpur, M. M. Watkins, and Ch. Reigber, Geophys. Res. Lett. **31**, L09607 (2004).
- [44] Ch. Reigber, R. Schmidt, F. Flechtner, R. König, U. Meyer, K.-H. Neumayer, P. Schwintzer, and S. Y. Zhu, J. Geodyn. **39**, 1 (2005).
- [45] J. Kim, P. Roeset, S. Bettadpur, B. D Tapley, and M. M. Watkins, in *IAG Symposium Series 123*, edited by M. Sideris (Springer, Berlin, 2001) p. 103.
- [46] B. D. Loomis, R. S. Nerem, and S. B. Luthcke, J. Geodesy, at press doi:10.1007/s00190-011-0521-8 (2011).
- [47] R. Pail, H. Goiginger, W.-D. Schuh, E. Höck, J. M. Brockmann, T. Fecher, T. Gruber, T. Mayer-Gürr, J. Kusche, A. Jäggi, and D. Rieser, Geophys. Res. Lett. **37**, L20314 (2010).
- [48] M. Burgay, N. D’Amico, A. Possenti, R. N. Manchester, A. G. Lyne, B. C. Joshi, M. A. McLaughlin, M. Kramer,

- J. M. Sarkissian, F. Camilo et al., *Nature* **426**, 531 (2003).
- [49] A. G. Lyne, M. Burgay, M. Kramer, A. Possenti, R. N. Manchester, F. Camilo, M. A. McLaughlin, D. R. Lorimer, N. D'Amico, B. C. Joshi et al., *Science* **303**, 1153 (2004).
- [50] M. Kramer, I. H. Stairs, R. N. Manchester, M. A. McLaughlin, A. G. Lyne, R. D. Ferdman, M. Burgay, D. R. Lorimer, A. Possenti, N. D'Amico et al., *Science* **314**, 97 (2006).
- [51] L. Iorio, *New Astron.* **14**, 40 (2009).
- [52] A. M. Ghez, S. Salim, N. N. Weinberg, J. R. Lu, T. Do, J. K. Dunn, K. Matthews, M. R. Morris, S. Yelda, E. E. Becklin et al., *Astrophys. J.* 689, 1044 (2008).
- [53] S. Gillessen, F. Eisenhauer, T. K. Fritz, H. Bartko, K. Dodds-Eden, O. Pfuhl, T. Ott, and R. Genzel, *Astrophys. J.* 707, L114 (2009).